जलवायु
JALAWAAYU
(Interdisciplinary Journal of Atmospheric and Hydrospheric Sciences)
Journal home page: https://cdhmtu.edu.np/journal/index.php/jalawaayu

Research Article

Observations and climate models confirm precipitation pattern is changing over Nepal

Rocky Talchabhadel [1, 2, 3 *]

[1] Texas A& M Agri Life Research, Texas A&M University, El Paso, TX, 79927, USA
[2] Smartphones For Water Nepal (S4W-Nepal), Lalitpur, 44700, Nepal
[3] Interdisciplinary Research Institute for Sustainability (IRIS), Kathmandu, 44600, Nepal

ARTICLE INFO

Received: 2 February 2021
Received in Revised form: 11 March 2021
Accepted: 12 March 2021
Available Online: 21 April 2021

Keywords

Climate model
Gauge-based observation
Precipitation indices
Shared Socioeconomic Pathway (SSP)

**Correspondence*

rocky.talchabhadel@ag.tamu.edu

Abstract: This paper presents a comprehensive picture of precipitation variability across Nepal over the present (1985-2014) and future (2021-2050) based on gauge-based observations from 28 precipitation stations distributed throughout the country and thirteen climate models of the latest Coupled Model Intercomparison Project Phase 6 (CMIP6) under two Shared Socioeconomic Pathways (SSP 245 and SSP 585). Seventeen different precipitation indices are computed using daily precipitation data based on gauge-based observations and climate models. Along with absolute extreme precipitation indices, such as maximum 1-day, maximum consecutive 3-day, 5-day, and 7-day precipitation amounts, this study also computes the contribution of such instances to the annual precipitation. The selected precipitation indices not only allow for the analyses of heavy precipitation-related extremes but also guide the evaluation of agricultural productivity and drought indications, such as consecutive dry and wet days (CDD and CWD). The number of wet days and average precipitation during those wet days, along with the information of

Cite this paper: Talchabhadel, R. (2021): Observations and climate models confirm precipitation pattern is changing over Nepal, JALAWAAYU, Vol. 1(1), 25-46.
DOI: https://doi.org/10.3126/jalawaayu.v1i1.36448

the number of days with daily precipitation ≥ 10, 20, 50, and 100 mm, summarize the distribution of total precipitation. This study emphasizes changing precipitation patterns by looking at these indices over the present and future periods. Observations and climate models show a changing nature of precipitation over Nepal. However, different climate models exhibit a different severity of changes. Though the yearly precipitation amount is not altered noticeably, this study finds that the extremes are expected to alter significantly than the averages. It is also to be noted that climate models are unable to capture localized extremes in Nepal Himalayas.

1. Introduction

Precipitation is one of the critical components of the hydrologic cycle. It varies spatially depending on several factors, including large-scale atmospheric circulation, local topography, and climate. Also, the precipitation fluctuates from year to year and over decades. The changes in frequency, amount, and intensity of precipitation affect society and the environment (Trenberth, 2011). Several studies report the precipitation pattern is changing rapidly and expected to alter more under the influence of climate change (Alexander, 2016; Hulme et al., 1998; Myhre et al., 2019; Wentz et al., 2007). Extremes are affected (are expected to alter) more than mean precipitation under changing climate (Berg et al., 2013; Kharin et al., 2013). However, the magnitude of alteration is uncertain (Allan & Soden, 2008; Allen & Ingram, 2002) and varies from region to region. Several studies attempt to unravel such precipitation alterations globally (Dore, 2005; Groisman et al., 1999), regionally (Klein-Tank et al., 2006), and at national (Bohlinger & Sorteberg, 2018; Kansakar et al., 2004; Talchabhadel et al., 2018) and basin scales (Dhaubanjar et al., 2020; Kaini et al., 2020; Talchabhadel et al., 2020).

Rising global temperatures are very likely to alter atmospheric moisture affecting atmospheric circulation and precipitation (Dore, 2005). Being a developing country and highly vulnerable to climate change, Nepal has several challenges in strengthening the adaptation capacity to a more significant climatic/weather variation. A sound understanding of precipitation variability would help manage and cope with the climate change effect. The historical tendency can be attributed based on gauge-based precipitation observations. And, future precipitation can be derived by looking at climate models' outputs. Global and regional climate models (GCM and RCM) inform projected future climate. They vary from model to model (Vecchi & Soden, 2007). Their performance should be checked with observed data at the historical period. Multiple models are analyzed to reduce uncertainty with climate models, and the ensemble of these models is often used to inform decisions (Kadel et al., 2018; Turner & Annamalai, 2012).

The working group on climate modeling established the Coupled Model Intercomparison Project (CMIP) in 1995 to better understand past, present, and future climate changes in a multi model context and provide standardized climate simulations and outputs. The CMIP recently entered into its sixth phase (i.e., CMIP6). The models have improved parameterization schemes for major biogeochemical and physical climate system processes (Eyring et al., 2016). Several modeling groups release their new simulations from CMIP5 to CMIP6 (e.g., Gusain et al., 2020; Kawai et al., 2019; Swart et al., 2019; Wu et al., 2019; Yukimoto et al., 2019). The CMIP6 uses a new set of shared socioeconomic pathways (SSPs) considering radiative forcings related to emissions, societal concerns, and land use scenarios (Cook et al., 2020). The representative concentration pathways (RCPs) only describe different greenhouse gases emissions and other radiative forcings that might occur in the future. They developed four pathways, spanning a range of forcing in 2100 (2.6, 4.5, 6.0, and 8,5 watts per meter squared), but did not include any socioeconomic factors. Based on CMIP5, several studies (Dhaubanjar et al., 2020; Kadel et al., 2018; Kaini et al., 2020; Rajbhandari et al., 2016; Talchabhadel et al., 2020) are conducted on assessing precipitation variability during historical and future periods in Nepal. These studies project future scenarios across the river basins or the entire country using CMIP5 models. Some studies (Aryal et al., 2019; Bhatta et al., 2019, 2020; Dahal et al., 2015; Pandey et al., 2019, 2020) simulate the future streamflow using the hydrologic model and climate models in different watersheds of the country. There are still no studies in Nepal using the CMIP6 outputs as they are new sets of data.

For the current study, two scenarios (SSP 2 and SSP 5) are considered. SSP 2 represents the middle of the road (i.e., intermediate challenges for mitigation and adaptation), whereas SSP 5 represents fossil-fueled development (i.e., high challenges for mitigation and low challenges for adaptation). This study uses the combination of SSP 2 with RCP 4.5 (SSP 245 hereinafter or medium forcing middle of the road pathway) and SSP 5 with RCP 8.5 (SSP 585 hereinafter or high end forcing pathway) for the analysis of projected data developed by Mishra et al. (2020). They developed daily bias-corrected precipitation data at a spatial resolution of 0.25^{o} for South Asia for thirteen CMIP6-GCMs for four scenarios (SSP 126, SSP 245, SSP 370, and SSP 585). This paper informs the precipitation variability across Nepal over the present (1985-2014) and future (2021-2050) using 28 high-quality precipitation observations and thirteen CMIP6-GCMs under SSP 245 and SSP 585. The chosen stations are homogenous, and they have >95% data availability with no sudden jumps and changes in observations. Also, these stations were selected considering adequate spatial coverage across the country. A total of seventeen precipitation indices is computed from daily precipitation data for both present and future periods. This study compares these indices between the present and future. The main objective of the study is to evaluate and quantify precipitation variation between two climatic phases (i.e., present and future) across the country using climate models.

2. Materials and Methods

This section describes the study domain. Also, materials used and methods adopted are discussed in this section.

2.1. Study domain

Figure 1a shows Nepal's location, situated on the southern slope of the central Himalayas in South Asia. The country is bounded by China on the north and India on the remaining sides. The elevation varies from 60 m above sea level (asl) to 8848.86 m asl (Mt. Sagarmatha, world's highest peak). Due to a sharp altitudinal difference in a short latitudinal distance, the country possesses diverse climate classes varying from tropical (in the south) to polar (in the north) (Karki et al., 2016). Figure 1b shows the location of 28 precipitation stations used in this study, and the color gradient used in the station indicates the mean annual precipitation from 1985 to 2014. The station at Pokhara shows the highest mean annual precipitation (i.e., 3868 ± 559.9 mm) and the station at Thakmarpha shows the least mean annual precipitation (i.e., 402 ± 72.1 mm) for the present period (1985-2014). A description of these stations is available in Table S1 in the supplementary materials. The arithmetic average of mean annual precipitation of these 28 precipitations is 1822 mm, which generally informs the country-averaged precipitation based on selected stations.

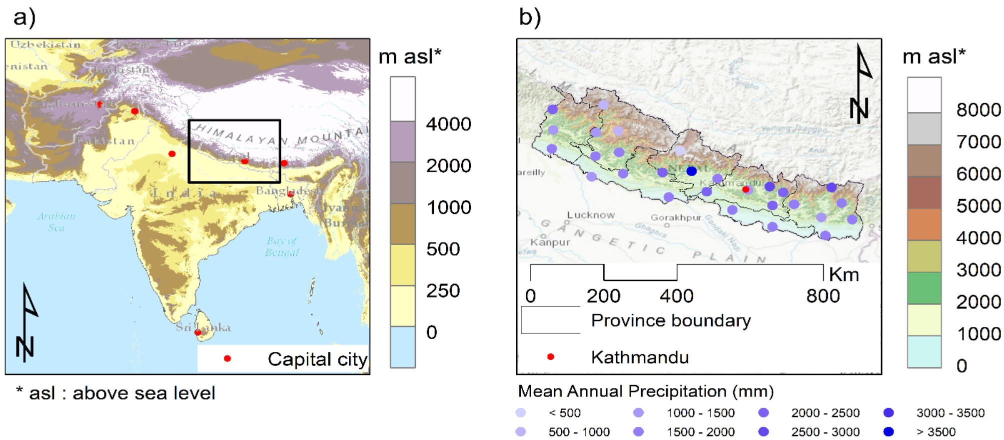

Figure 1. a) Location of Nepal in South Asia. The red dot shows the capital city. b) Location of 28 precipitation stations used in this study, and the color gradient of these stations informs the mean annual precipitation for the present period (1985 – 2014). The shaded background is the topography of the country.

2.2. Precipitation data and indices used

The daily precipitation data were acquired from 1985 to 2014 from the Department of Hydrology and Meteorology (DHM) for the present period. Table 1 shows a summary of the climate models used in this study. Different resolution GCMs (varying from 0.7° to >2°) were bias-corrected using Empirical Quantile Mapping (EQM) for 1951-2014 and projected for 2015-2100 by Mishra et al. (2020) at a spatial resolution of 0.25°. Daily precipitation data from the climate models were extracted at 28 precipitation station locations for historical (1985-2014) and future (2021-2050) in this study.

Table 1. Climate models used in this study

SN	Model name	Country	GCM resolution
1	ACCESS-CM2	Australia	1.25^{o} x 1.875^{o}
2	ACCESS-ESM1-5		1.25^{o} x 1.875^{o}
3	BCC-CSM2-MR	China	1.1215^{o} x 1.125^{o}
4	CanESM5	Canada	2.7906^{o} x 2.8125^{o}
5	EC-Earth3	Europe-wide consortium	0.7018^{o} x 0.703125^{o}
6	EC-Earth3-Veg		0.7018^{o} x 0.703125^{o}
7	INM-CM4-8	Russia	1.5^{o} x 2.0^{o}
8	INM-CM5-0		1.5^{o} x 2.0^{o}
9	MPI-ESM1-2-LR	Germany	0.9351^{o} x 0.9375^{o}
10	MPI-ESM1-2-HR		1.8653^{o} x 1.875^{o}
11	MRI-ESM2-0	Japan	1.1215^{o} x 1.125^{o}
12	NorESM2-LM	Norway	1.8947^{o} x 2.5^{o}
13	NorESM2-MM		0.9424^{o} x 1.25^{o}

I computed the precipitation indices (shown in Table 2) from gauge-based observations and climate models' outputs. Table 1 shows how each of the precipitation indices is calculated. CDD and CWD are duration-based indices referring to maximum lengths of consecutive dry and wet days in a year, respectively. They provide valuable information on likely droughts and antecedent soil moisture. R1 is the number of wet days in a year, PRCPTOT is total precipitation in those wet days in a year, and SDII is average precipitation in wet days. R10, R20, R50, and R100 are threshold-based indices that inform the yearly count of days when daily precipitation ≥ 10, 20, 50, and 100 mm, respectively. Similarly, RX1day, RX3day, RX5day, and RX7day are absolute indices of extreme precipitation which inform the maximum 1-day, maximum consecutive 3-day, 5-day, and 7-day precipitation amount, respectively. RX1day(%), RX3day(%), RX5day(%), and RX7day(%) are ratio-based indices that inform the contribution of these absolute extreme precipitation indices to the annual precipitation in a year. These ratio-based indices help design and plan an early warning system of rainfall-induced shallow landslides, as these landslides typically occur during such instances.

Table 2. Precipitation indices used in this study

ID	Indicator name	Definitions	Units
CDD	Consecutive dry days	Maximum number of consecutive days with PRCP[1] < 1 mm	days
CWD	Consecutive wet days	Maximum number of consecutive days with PRCP[1] ≥ 1 mm	days
R1	Number of wet days	Annual count of days when PRCP[1] ≥ 1 mm	days
PRCPTOT	Annual total wet-day precipitation	Annual total precipitation in wet days (PRCP[1] ≥ 1 mm)	mm
SDII	Simple daily intensity index	Average precipitation in wet days (PRCPTOT/R1)	mm/day
R10	Number of slightly heavy precipitation days	Annual count of days when PRCP[1] ≥ 10 mm	days
R20	Number of heavy precipitation days	Annual count of days when PRCP[1] ≥ 20 mm	days
R50	Number of very heavy precipitation days	Annual count of days when PRCP[1] ≥ 50 mm	days
R100	Number of extremely heavy precipitation days	Annual count of days when PRCP[1] ≥ 100 mm	days
RX1day	Max 1-day precipitation	Yearly maximum 1-day precipitation	mm
RX3day	Max consecutive 3-day precipitation	Yearly maximum consecutive 3-day precipitation	mm
RX5day	Max consecutive 5-day precipitation	Yearly maximum consecutive 5-day precipitation	mm
RX7day	Max consecutive 7-day precipitation	Yearly maximum consecutive 7-day precipitation	mm
RX1day(%)		Ratio of RX1day with PRCPTOT	%
RX3day(%)		Ratio of RX3day with PRCPTOT	%
RX5day(%)		Ratio of RX5day with PRCPTOT	%
RX7day(%)		Ratio of RX7day with PRCPTOT	%

[1]*PRCP: daily precipitation*

The performance of climate models was checked with gauge-based observations during the historical period (1985-2014). I applied several error metrics, such as normalized root mean square error (nRMSE), normalized standard deviation (nSD), and correlation coefficient (R), to quantify the climate models' performances.

$$nRMSE = \frac{\sqrt{\frac{\Sigma\left(obs - CM\right)^2}{N}}}{\overline{Obs}} \quad (1)$$

$$nSD = \frac{SD_{CM}}{SD_{Obs}} = \frac{\sqrt{\frac{\Sigma\left(CM - \overline{CM}\right)^2}{N}}}{\sqrt{\frac{\left(Obs - \overline{Obs}\right)^2}{N}}} \quad (2)$$

$$R = \frac{\Sigma\left(Obs - \overline{Obs}\right)\left(CM - \overline{CM}\right)}{\sqrt{\Sigma\left(Obs - \overline{Obs}\right)^2}\sqrt{\Sigma\left(CM - \overline{CM}\right)^2}} \quad (3)$$

where, *Obs* and *CM* are annual precipitation based on observed and climate models, respectively. *Obs* and *CM* denote mean annual precipitation for the historical period (i.e., 1985-2014) based on observed and climate models, respectively, and *N* is the number of years. Root mean square error (*RMSE*) is a popular indicator for quantifying the absolute error at any station. Here, the *RMSE* is normalized using observational average, and *nRMSE* is computed. *nRMSE* = 1 represents that the error is equivalent to the observational average. Similarly, simulated standard deviation (*SD*) is normalized using observational SD, and *nSD* is computed. *nSD* = 1 represents that the simulated interannual deviation is congruous to observational interannual variation. Here, *R* represents the correlation between observational and simulated annual precipitation. *R*= 1 represents a perfect correlation, indicating similar year-to-year fluctuations. This study currently limits a further bias-correction of the precipitation data, developed by Mishra et al. (2020). For this study, deviations in the future period were computed with respect to each climate model's historical period for all precipitation indices. Likely change of precipitation indices would help understand the possible impacts of climate change on precipitation variability under selected SSPs.

3. Results

This section presents key results from the analysis of precipitation indices and their shifts from the present to the future. At first, the performance of climate models is demonstrated by comparing with gauge-based observations.

3.1. Performance of climate models with respect to gauge-based observations

Figure 2 shows performance evaluation at different stations for different climate models during the historical period based on selected performance metrics. Concerning *nRMSE*, this study finds that all climate models show a similar value for the country-averaged precipitation (an average of 0.42 ranging from 0.38 by BCC-CSM2-MR to 0.46 by CanESM5), indicating that the *RMSE* value is about 40% of the observed mean annual precipitation (i.e., approx. 750 mm). However, there is a substantial station-wise variation. The ensemble of 13 climate models shows that *nRMSE* ranges from 0.24 (Okhaldhunga and Taplejung) to 1.27 (Thakmarpha).

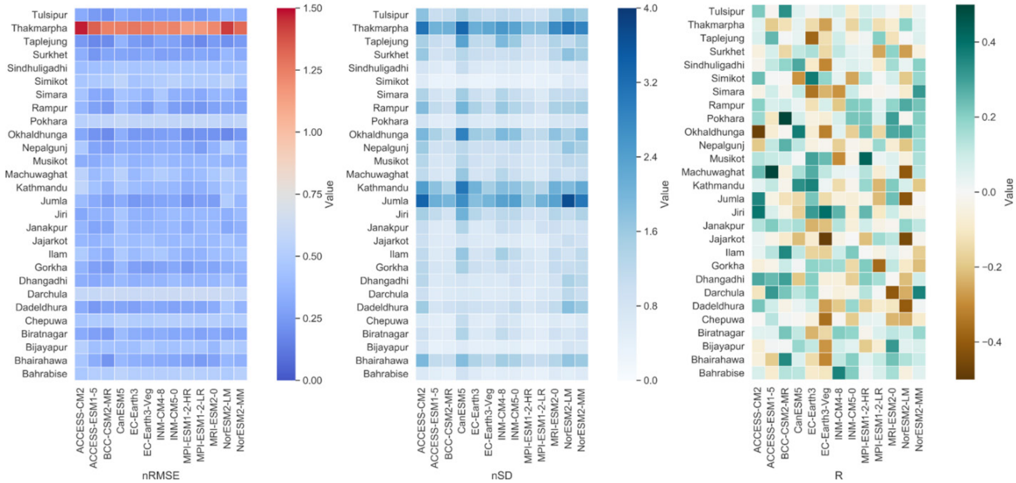

Figure 2. Performance evaluation at different stations for different climate models during the historical period (1985-2014) based on nRMSE, nSD, and R. nRMSE: normalized root mean square error, nSD: normalized standard deviation, and R: correlation coefficient.

The climate models show the mean annual precipitation of Okhaldhunga is about 1643 mm (varying from 1569 mm by CanESM5 to 1824 mm by ACCESS-CM2), which almost equals the observed one (i.e., 1785 mm). Similarly, the climate models show the mean annual precipitation of Taplejung is about 1880 mm (varying from 1789 mm by MPI-ESM1-2-HR to 2039 mm by ACCESS-CM2), which almost equals the observed one (i.e., 1970 mm). Climate models effectively simulate mean annual precipitation for these stations, with the *RMSE* value equals about 25% of the observed mean annual precipitation. However, five stations (namely, Bahrabise, Chepuwa, Darchula, Pokhara, and Thakmarpha) show $nRMSE > 0.5$, meaning *RMSE* value is greater than 50% of the observed mean annual precipitation. Climate models show that the RMSE is greater than the observed mean annual precipitation at Thakmarpha (an average value of nRMSE is 1.27, varying from 1.23 by INM-CM5-0 to 1.47 by ACCESS-CM2). The climate models show the mean annual precipitation of Thakmarpha is about 875 mm (ranging from 841 mm by MPI-ESM1-2-HR to 948 mm by ACCESS-CM2), which is greater than twice the observed one (i.e., 402 mm), indicating a substantial overestimation. In contrast, the observed mean annual precipitation at Pokhara is around 4000 mm whereas, all climate models simulate almost half of the observed precipitation, indicating a significant underestimation. Even the coarse-resolution GCMs were downscaled and bias-corrected at 0.25^{o} by Mishra et al. (2020), they could not replicate a ground reality of spatial variability for Nepal. The highest rainfall pocket like Pokhara is highly underestimated, whereas the drier region like Thakmarpha is substantially overestimated by the climate models. This evidence suggests carrying a local-specific bias correction of these climate models to use absolute precipitation values. However, as the current study focuses on likely shifts in the future with respect to the present period, a relative deviation for each climate model is carried out by comparing with historical data of the same climate model. The heat map for *nRMSE* in Figure 2 shows how each climate model performs at each station. Except for Thakmarpha station, the values are in range of 0.18 (Taplejung by ACCESS-ESM1-5) to 0.63 (Darchula by MRI-ESM2-0).

Concerning *nSD*, climate models show a range of values for the country-averaged precipitation (an average of 1.1 ranging from 0.8 by MPI-ESM1-2-LR to 1.54 by CanESM5), indicating that the interannual variation is captured differently by different models. The ensemble of 13 climate models shows that *nSD* ranges from 0.41 (Simikot) to 2.5 (Thakmarpha). The climate models show the *SD* of annual precipitation of Simikot is about 172 mm (varying from 119 mm by MPI-ESM1-2-HR to 268 mm by NorESM2-LM), which almost equals half of the observed one (i.e., 417 mm). Based on the ensemble climate model, two stations (Jumla and Thakmarpha) show $nSD > 2$, meaning the interannual variation of these two stations is substantially high than the observed *SD* of annual precipitation. As mentioned above, the climate models overestimate in the drier region of the country. In the case of Jumla, the climate models are better at simulating the mean annual precipitation but fail to replicate the interannual variation. The climate models show the mean annual precipitation of Jumla is about 912 mm (ranging from 866 mm by MPI-ESM1-2-HR to 994 mm by NorESM2-LM), which is not so high compared to the observed one (i.e., 800 mm). However, the climate models show the *SD* of annual precipitation of Jumla is about 200 mm (varying from 135 mm by MPI-ESM1-2-HR to 306 mm by NorESM2-LM), which almost equals double of the observed one (i.e., 82 mm). The heat map for *nSD* in Figure 2 shows how each climate model performs at each station. The values range from 0.29 (Simikot by MPI-ESM1-2-HR) to 3.71 (Jumla by NorESM2-LM). For Simikot, the climate models show the mean annual precipitation is about 788 mm (ranging from 749 mm by MPI-ESM1-2-HR to 856 mm by NorESM2-LM), which is not so low compared to the observed one (i.e., 962 mm). However, the climate models show the *SD* of annual precipitation of Simikot is about 171 mm (varying from 119 mm by MPI-ESM1-2-HR to 268 mm by NorESM2-LM), which almost equals half of the observed one (i.e., 417 mm). This evidence shows that even though climate models depict the mean annual precipitation of the station, they often fail to replicate the interannual variation. For a year-to-year correlation, this study looks into the value of the correlation coefficient (*R*). Concerning *R*, all climate models show overall poor correlation ($-0.3 < R < 0.3$) at all stations, except a few. The heat map for *R* in Figure 2 shows how each climate model performs at each station. The values range from -0.48 (Jajarkot by EC-Earth3-Veg) to 0.51 (Pokhara by BCC-CSM2-MR). It is quite clear that the climate models could not replicate the year-to-year variation.

3.2. Yearly variation of precipitation indices based on gauge-based observations and multi model mean of climate models

Figure 3 shows yearly variations of different precipitation indices for present and future periods. Based on a multi model mean of 13 climate models, the interannual variation is expected to be moderate for all precipitation indices. As indicated earlier that the climate models are unable to replicate the local extremes. Therefore, the yearly prediction might not be certain enough. However, the general tendency and expected deviation with respect to the historical data would surely provide insights into these indices' likely deviations. Overall country-wide average (i.e., the arithmetic average of 28 stations) for all precipitation indices show greater value during the future period than the historical period. A slightly bigger deviation could be expected under SSP 585 than SSP 245. The degree of variation, however, is different for different precipitation indices. Also, some stations show a negative deviation for some precipitation indices. The detail on these deviations is presented in the subsequent section.

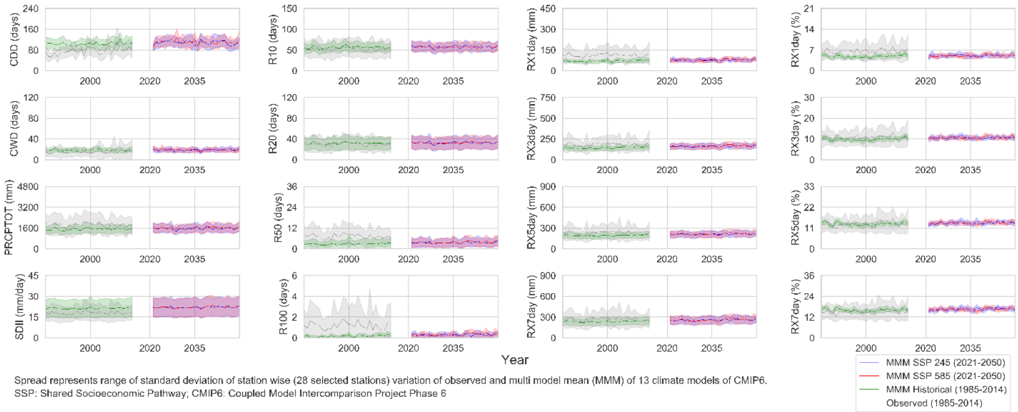

Figure 3. Yearly variation of different precipitation indices based on gauge-based observations (gray) and a multi model mean of 13 climate models of CMIP6 (green for historical, blue for SSP 245, and red for SSP 585). A description of the precipitation indices is shown in Table 2.

An increasing CDD is expected to continue in the future, similar to what it shows during the present period. Therefore, dry spells could increase in the coming days affecting badly to winter crops. Simultaneously, CWD and PRCPOT show a slightly rising trend, indicating a wetter scenario in the future period than the present. One could anticipate a wetter monsoon period, whereas a drier winter season, resulting in a slightly increasing total annual precipitation in the future. The total number of wet days (R1) is expected not to increase substantially. But, SDII is projected to increase notably. Meaning, the number of rainy days would be more or less constant, but these rainy days would produce more heavy rains, indicating a pronounced extreme precipitation effect. The number of heavy, very heavy, and extremely heavy precipitation days (R20, R50, and R100) are anticipated to increase in the coming days. A similar tendency could be seen for the absolute extreme precipitation indices (RX1day, RX3day, RX5day, and RX7day). As a result, ratio-based indices, such as RX1day(%), RX3day(%), RX5day(%), and RX7day(%), show a higher contribution of these extreme instances to annual precipitation (PRCPTOT). This evidence highlight the severity of extreme precipitation would increase in the future.

3.3. Station-wise yearly variation of selected precipitation indices based on gauge-based observations and climate models

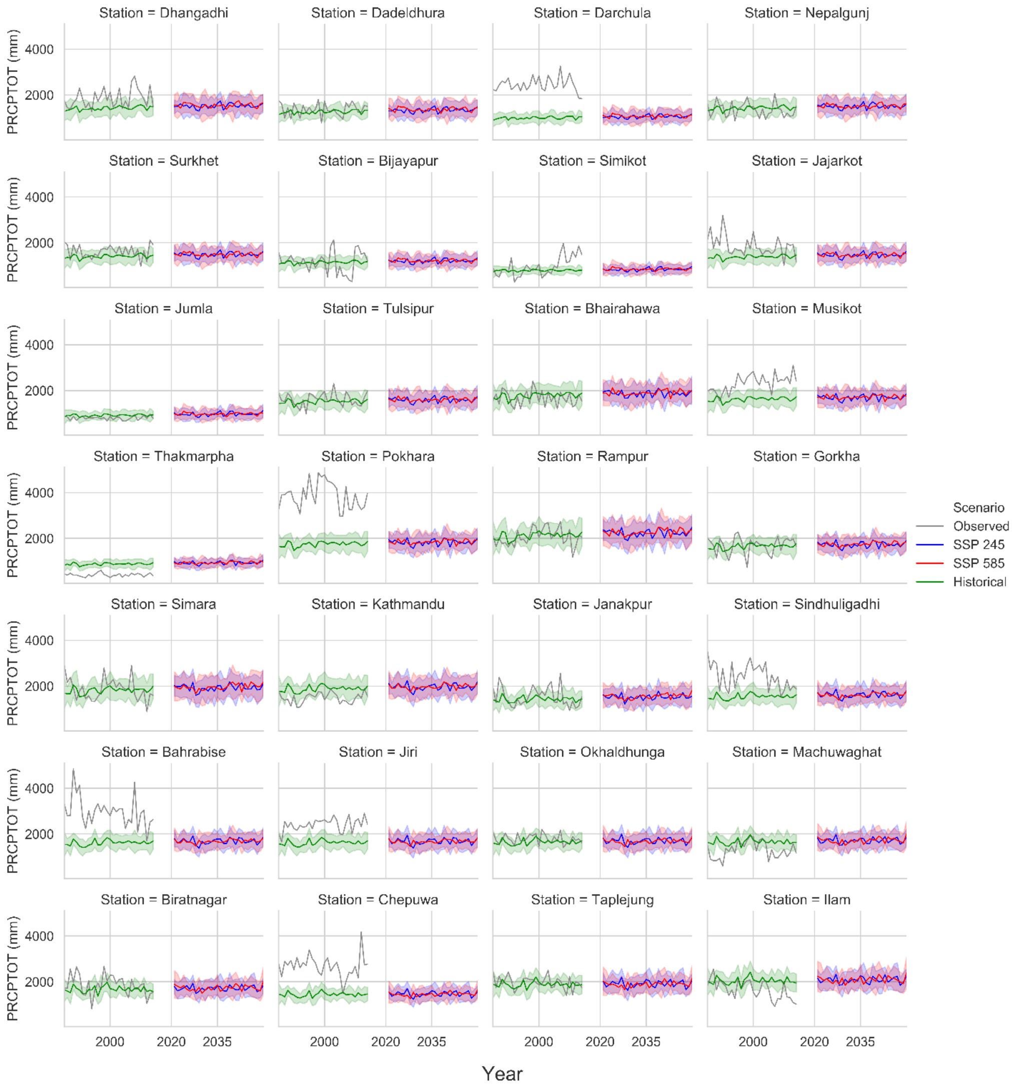

Figure 4. Yearly variation of PRCPTOT (Annual total precipitation) at 28 precipitation stations based on gauge-based observations (gray) and 13 climate models of CMIP6 (green for historical, blue for SSP 245, and red for SSP 585). Spread for climate models shows the range of standard deviation.

This section presents a station-wise interannual variation of selected precipitation indices (i.e., PRCPTOT, R1, RX1day, and RX7day) in Figures 4, 5, 6, and 7, respectively. As mentioned earlier, localized precipitation variability could not be replicated by the climate models. However, a general tendency is depicted, and normal values of PRCPTOT are congruent at most stations except a few, such as Pokhara, Bahrabise, Chepuwa, and Darchula (refer to Figure 4). It highlights a need for local-level bias correction and incorporation of that correction factors during projected periods.

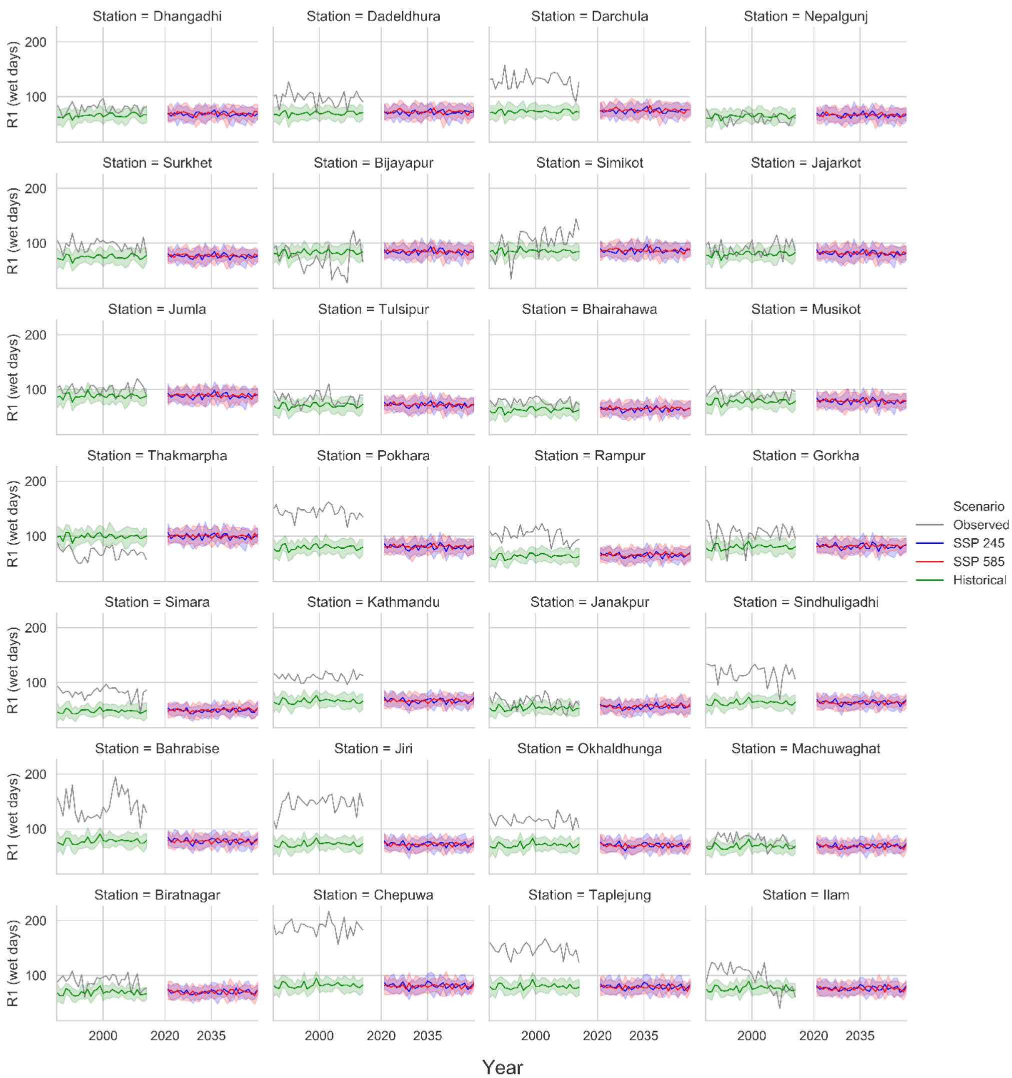

Figure 5. Same as Figure 4 but for R1 (Annual total wet days)

This study emphasizes the deviation of these precipitation indices in the future period with respect to the historical period of the individual climate model. Thus, the likely proportional deviations are not much affected. Different climate models project a diverse range of future projections. Under both SSPs, a similar interannual variation is expected. Climate models show a notable underestimation of the number of wet days in the historical period at most stations, such as Darchula, Pokhara, Rampur, Simara, Kathmandu, Sindhuligadhi, Bahrabise, Jiri, Okhaldhunga, Chepuwa, and Taplejung (refer to Figure 5).

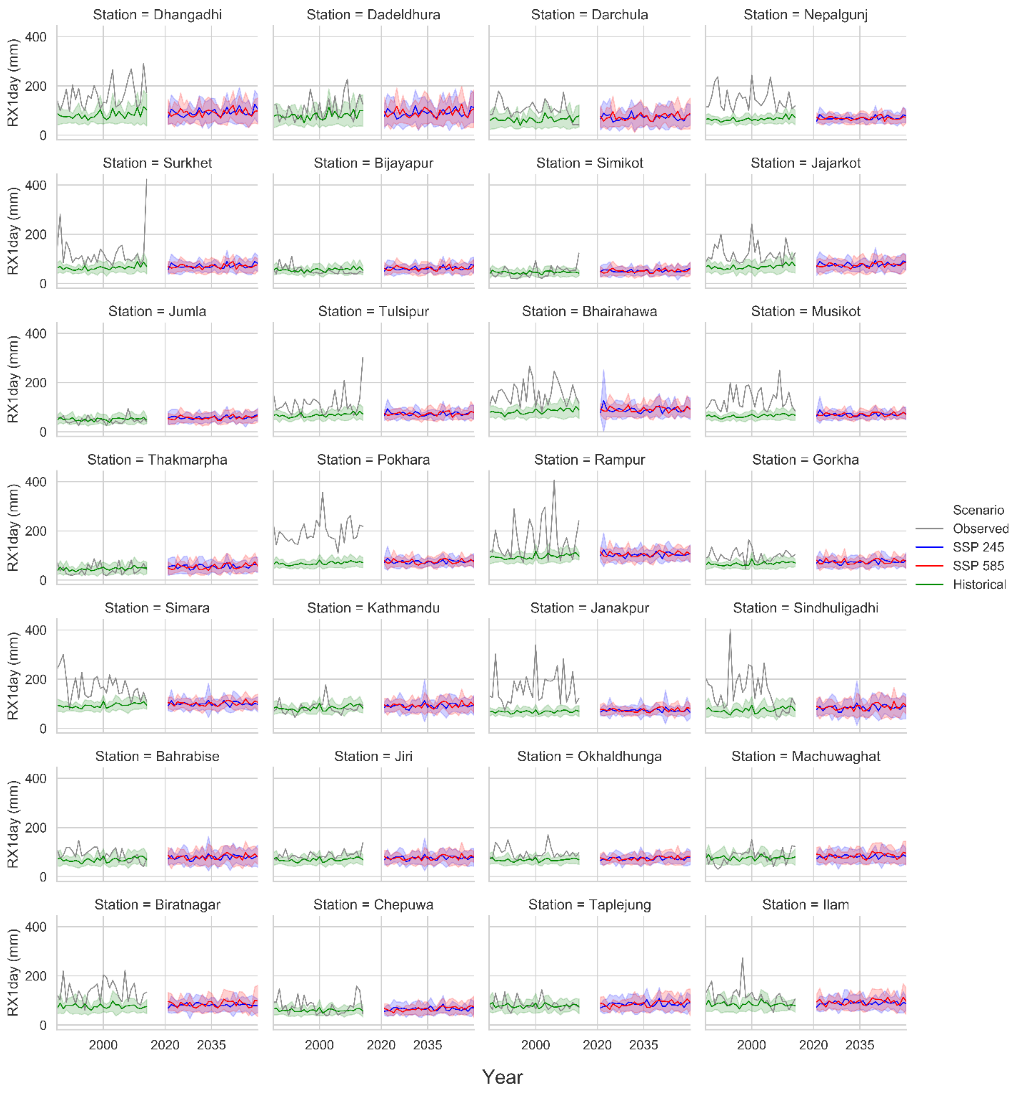

Figure 6. Same as Figure 4 bur for RX1day (Yearly maximum 1-day precipitation)

It infers that a scaling method of bias correction would not solve missing rain events. Because by employing the correction factors, the precipitation quantity could be corrected, and biases could be reduced, but it would be challenging to convert non-rainy days to rainy days. Climate models often miss slight to small precipitation (i.e., daily precipitation < 10 mm) events.

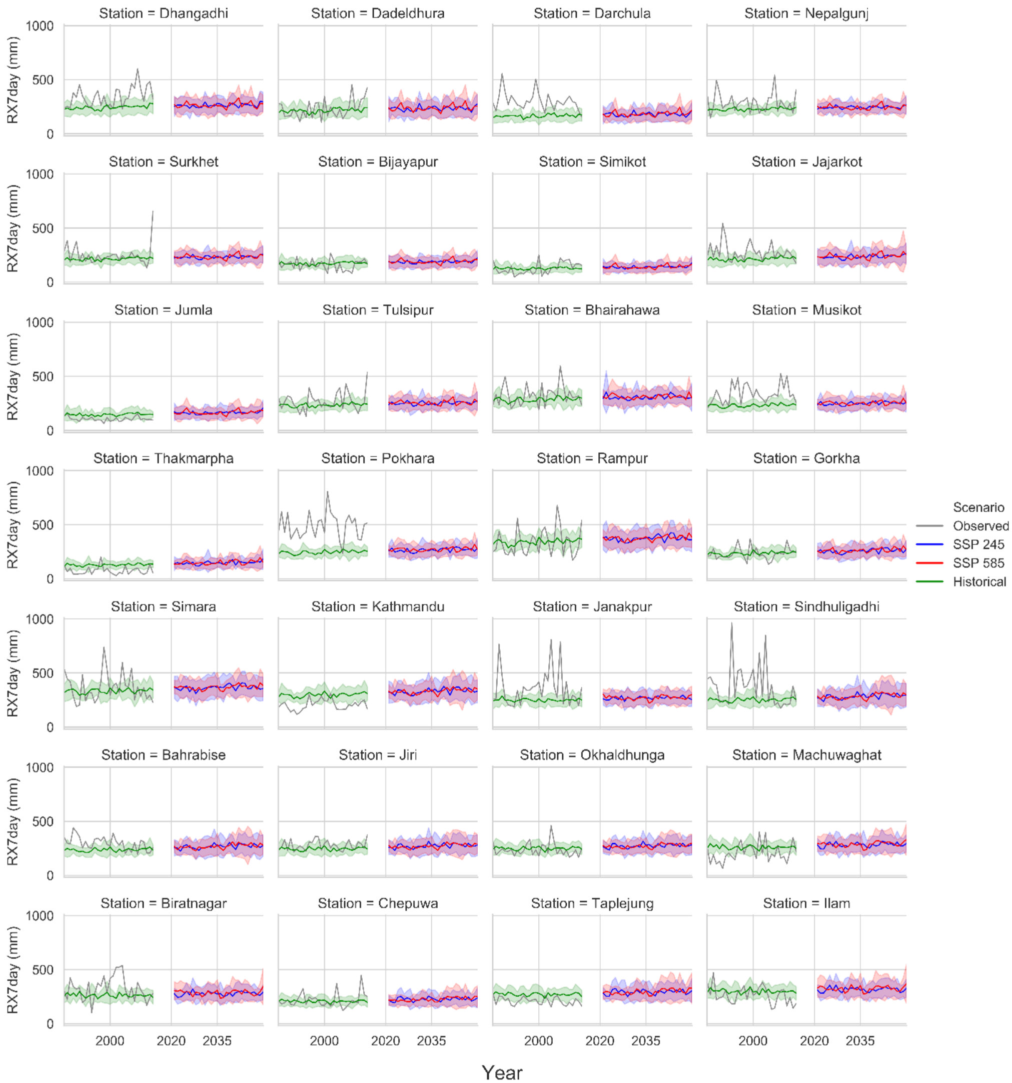

Figure 7. Same as Figure 4 but for RX7day (Yearly maximum consecutive 7-day precipitation)

Based on the projected deviation of the number of wet days, it is found that there is not much alteration in the future period with respect to the historical period. Both SSPs show a similar nature of fluctuation of R1. Figures 6 and 7 also highlight that climate models cannot mimic the extreme local precipitation at most stations. It is a great challenge to replicate extreme using climate models. However, they show that the future would have a certain higher extreme than the present period. And, it is more pronounced under SSP 585 than SSP 245.

3.4. Projected changes of precipitation indices

Figure 8 shows deviations of different country-averaged precipitation indices during the future period with respect to the historical period based on different climate models.

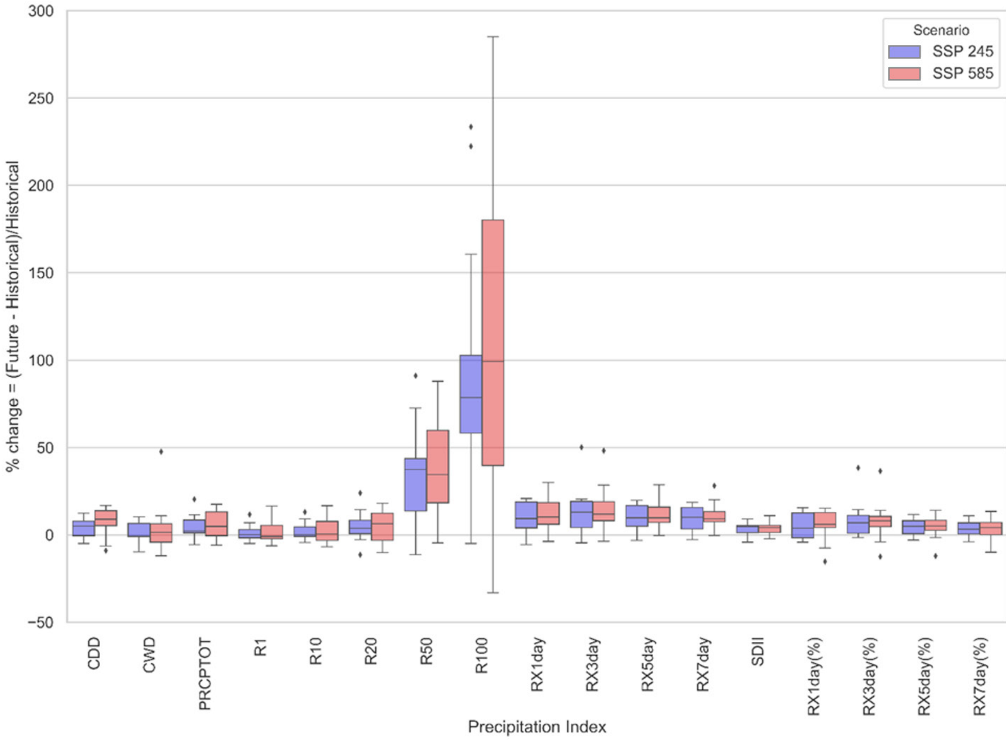

Figure 8. Boxplot showing the percentage change of country-averaged different precipitation indices in the future period (2021-2050) with respect to the historical period (1985-2014) under changing climate based on 13 climate models under two Shared Socio-economic Pathways (SSPs). The box plot shows quantiles (Q1 and Q3), median (Q2), and range of climate model variation. A description of the precipitation indices is shown in Table 2. Here deviation is computed as a difference of normal values between future and historical periods with respect to the historical period expressed in %. A positive value represents increasing value in the future, whereas a negative value represents decreasing value in the future with respect to the historical period.

Under SSP 585, the intermodal variability is larger compared to SSP 245. The climate models' ensemble also shows that a larger deviation is expected under SSP 585 than SSP 245. R50 and R100 are expected to increase substantially with respect to the historical period. A few models show some negative deviation, whereas most models show positive deviation for all precipitation indices—for instance, CanESM5, MPI-ESM1-2-LR, and NorESM2-MM project PRCPTOT to negatively deviate under SSP 245. Similarly, BCC-CSM2-MR, MPI-ESM1-2-HR, MPI-ESM1-2-LR, and NorESM2-

MM anticipate PRCPTOT to shift negatively under SSP 585. The remaining all climate models project PRCPTOT to shift positively. In the case of CDD, four climate models (namely, ACCESS-CM2, CanESM5, EC-Earth3-Veg, and INM-CM5-0) anticipate negative deviation under SSP 245. Similarly, three climate models (namely, CanESM5, EC-Earth3-Veg, and NorESM2-LM) expect negative deviation. The remaining all climate models predict CDD to shift positively. In the case of CWD, seven (six) climate models expect negative deviation under SSP 245 (SSP 585), inferring the likely shift of CWD is less in the future under changing climate. Table 3 summarizes the possible deviation of different precipitation indices in the future period with respect to the historical period based on the multi model mean of 13 climate models.

Table 3. Projected deviation of different precipitation indices under changing climate based on multi model mean of 13 climate models. A description of the precipitation indices is shown in Table 2. Here deviation is computed as a difference of normal values between future (2021-2050) and historical (1985-2014) periods with respect to the historical period expressed in %. A positive value represents increasing value in the future, whereas a negative value represents decreasing value in the future with respect to the historical period.

	Based on 28 stations	**CDD**	**CWD**	**PRCP TOT**	**R1**	**R10**	**R20**	**R50**	**R100**	**SDII**
SSP245	Min	2.0	-2.5	1.6	-0.5	-1.0	-1.1	13.1	27.3	1.8
	Max	7.7	9.6	7.5	4.2	5.6	27.0	96.3	160.0	6.1
	Mean	4.3	1.5	4.9	1.3	2.0	5.5	36.1	81.3	3.6
SSP585	Min	4.3	-5.8	0.8	-1.6	-2.0	-1.7	14.8	26.9	2.5
	Max	10.3	13.1	9.4	6.4	7.4	26.8	92.5	200.0	6.1
	Mean	6.8	2.5	5.7	1.9	2.7	5.9	38.3	102.1	3.8

	Based on 28 stations	**RX1 day**	**RX3 day**	**RX5 day**	**RX7 day**	**RX1day (%)**	**RX3day (%)**	**RX5day (%)**	**RX7day (%)**
SSP245	Min	6.4	10.2	7.1	5.8	-1.7	3.2	-0.6	-0.5
	Max	21.3	22.3	16.2	15.1	14.0	14.6	9.0	7.9
	Mean	10.5	13.8	10.3	9.6	4.5	7.9	4.4	3.7
SSP585	Min	5.8	10.7	8.5	7.7	-1.9	2.3	-1.1	-1.1
	Max	21.0	22.6	17.8	17.1	13.0	14.0	9.5	8.8
	Mean	11.9	14.9	11.5	10.8	5.1	8.0	4.6	3.9

The deviations are mixed at various stations for different precipitation indices. However, for some indices, all stations reveal a positive deviation, such as CDD, PRCPTOT, R50, R100, SDII, RX1day, RX3day, RX5day, RX7day, and RX3day (%). It infers that these indices are likely to increase throughout the country. These indices include annual total precipitation, dry spells days, extreme precipitation amount and days, and average precipitation amount during rainy days. Although other indices have some negative deviations at a few stations, the overall country-wide scenario shows a positive deviation of all these precipitation indices. The severity of likely deviation is different for different precipitation indices. A bigger percentage change is expected for threshold-based extreme precipitation indices, such as R50, and R100 followed by absolute extreme precipitation indices, such as RX1day, RX3day, RX5day, and RX7day. The least deviation is projected for R1, meaning the number of wet days is likely to be unaffected in the coming days.

4. Discussion

Upon comparing the mean annual precipitation of different climate models with the observed value during the historical period, this study finds that CanESM5, MPI-ESM1-2-HR, and MPI-ESM1-2-LR represent drier climate models and ACCESS-CM2, ACCESS-ESM1-5, and NorESM2-LM denote wetter climate models for Nepal. However, the ensemble of selected thirteen climate models developed by Mishra et al. (2020) still underestimates the precipitation total for Nepal. The year-to-year correlation is very poor, suggesting a larger uncertainty on yearly analyses because all climate models have distinctive weaknesses in simulating different variables (Pincus et al., 2008; Schaller et al., 2011). One could expect even larger uncertainty on daily, monthly and seasonal scales. For a deviation analysis between climatic periods, normal values provide an insightful indication. Drier regions of the country are overestimated, whereas wetter regions are underestimated by most climate models in Nepal. Thus coarse-gridded GCMs are unable to replicate local precipitation variability. For a precise hydroclimatic analysis, local-level bias corrections are necessary. This study computes a relative deviation of different precipitation indices between historical and future periods for each climate model to reduce the errors with respect to observed values. Even though anticipated deviations are mixed at various stations for different precipitation indices based on different climate models, this study finds some indication of likely deviations. However, future projections are still difficult to provide with certainty (Trenberth et al., 2003). Extreme precipitation indices are likely to increase throughout the country compared to the annual precipitation and total wet days. The results are parallel with several studies, such as Donat et al. (2016), Fischer & Knutti (2016), and Allan & Soden (2008). A larger deviation is anticipated for threshold-based extreme precipitation indices, such as R50, and R100 followed by absolute extreme precipitation indices, such as RX1day, RX3day, RX5day, and RX7day. Therefore, the climate models inform a changing nature of precipitation in the coming days with more localized extremes but unchanged annual precipitation. One could expect more intense and more frequent precipitation extremes (Kharin et al., 2013) even seasonal and annual precipitation do not change that much. Changing precipitation patterns will impact livelihood and food security. The deviations are expected to be more pronounced under SSP 585 than SSP 245, suggesting to plan and move on lesser fossil-fueled development framework as much as possible.

5. Conclusions

This study reveals a shifting nature of precipitation variability across Nepal in the coming days with respect to the present period. Thirteen CMIP6 models under SSP 245 and SSP 585 are utilized to project future precipitation at 28 precipitation stations. Although climate models cannot replicate year-to-year variation and local extremes, this study carried out a relative change in the future with respect to the historical period. Several precipitation indices are diagnosed in this study. This study highlights that the extremes are anticipated to alter substantially than the averages. Climate models could not replicate year-to-year variation and magnitude, as depicted by performance metrics, such as nRMSE, nSD, and R. For instance, the highest rainfall pocket like Pokhara is highly underestimated. In contrast, the drier region like Thakmarpha is substantially overestimated by the climate models.

All climate models show a similar *nRMSE* value for the country-averaged precipitation (an average of 0.42 ranging from 0.38 by BCC-CSM2-MR to 0.46 by CanESM5), indicating that the *RMSE* value is about 40% of the observed mean annual precipitation (i.e., approx. 750 mm). CanESM5, MPI-ESM1-2-HR, and MPI-ESM1-2-LR represent drier climate models. And ACCESS-CM2, ACCESS-ESM1-5, and NorESM2-LM denote wetter climate models for Nepal. Different models project differently in the future, ranging from negative to positive deviation. However, most climate models anticipate a positive deviation of all precipitation indices. A substantial shift in R50 and R100 is projected, inferring heavy rainy days could increase in the coming days. Also, RX1day, RX3day, RX5day, and RX7day are anticipated to increase by more than 10%. These instances are mostly responsible for flash floods, riverine floods, and landslides. PRCPTOT is projected to increase slightly. However, the number of wet-days is not expected to alter. Overall, climate models reveal erratic precipitation would happen more frequently. Rising precipitation extremes and changing precipitation patterns should be considered while developing climate change adaptation strategies in the coming days.

Acknowledgments: The author would like to express his sincere gratitude to the Department of Hydrology and Meteorology (DHM), Government of Nepal, for providing the daily precipitation data. The author is grateful to Mishra et al. (2020) for sharing the bias-corrected CMIP6 data of 13 climate models for South Asia, including Nepal.

Conflicts of Interest: The author declares no conflict of interest.

Supplementary materials:

Table S1. Precipitation stations used in this study. The mean annual precipitation and standard deviation are computed from the annual precipitation from 1985 to 2014.

SN	Station ID	Name	Longitude	Latitude	Elevation (m asl)	Mean annual precipitation (mm) ± Standard deviation
1	209	Dhangadhi	80.6	28.8	187	1856.5 ± 397.0
2	104	Dadeldhura	80.6	29.3	1848	1366.3 ± 266.7
3	107	Darchula	80.6	29.9	1097	2449.5 ± 305.9
4	416	Nepalgunj	81.5	28.1	144	1357.7 ± 303.9
5	406	Surkhet	81.6	28.6	720	1623.5 ± 273.2
6	309	Bijayapur	81.6	29.2	1814	1154.0 ± 460.6
7	311	Simikot	81.8	30.0	2818	962.2 ± 417.9
8	404	Jajarkot	82.2	28.7	1231	1863.1 ± 441.4

9	303	Jumla	82.2	29.3	2366	800.6 ± 82.5
10	508	Tulsipur	82.3	28.1	725	1617.7 ± 278.1
11	705	Bhairahawa	83.4	27.5	109	1667.3 ± 312.9
12	722	Musikot	83.3	28.2	1280	2325.4 ± 366.2
13	604	Thakmarpha	83.7	28.8	2566	402.7 ± 72.1
14	804	Pokhara	84.0	28.2	827	3868.7 ± 559.9
15	902	Rampur	84.4	27.7	173	2058.5 ± 368.4
16	809	Gorkha	84.6	28.0	1097	1684.8 ± 358.9
17	909	Simara	85.0	27.2	130	1866.4 ± 467.3
18	1030	Kathmandu	85.4	27.7	1337	1489.9 ± 223.2
19	1111	Janakpur	86.0	26.7	90	1539.2 ± 414.5
20	1107	Sindhuligadhi	86.0	27.3	1463	2440.1 ± 537.5
21	1027	Bahrabise	85.9	27.8	850	2977.2 ± 637.5
22	1103	Jiri	86.2	27.6	2003	2404.7 ± 280.3
23	1206	Okhaldhunga	86.5	27.3	1720	1785.1 ± 207.6
24	1322	Machuwaghat	87.2	27.0	158	1302.5 ± 359.7
25	1319	Biratnagar	87.3	26.5	72	1852.5 ± 431.5
26	1317	Chepuwa	87.4	27.8	2590	2676.3 ± 457.3
27	1405	Taplejung	87.7	27.4	1732	1970.2 ± 273.7
28	1407	Ilam	87.9	26.9	1208	1653.8 ± 402.1

References

Alexander, L. V. (2016). Global observed long-term changes in temperature and precipitation extremes: A review of progress and limitations in IPCC assessments and beyond. *Weather and Climate Extremes*, *11*, 4–16. https://doi.org/10.1016/j.wace.2015.10.007

Allan, R. P., & Soden, B. J. (2008). Atmospheric Warming and the Amplification of Precipitation Extremes. *Science*, *321*(5895), 1481–1484. https://doi.org/10.1126/science.1160787

Allen, M. R., & Ingram, W. J. (2002). Constraints on future changes in climate and the hydrologic cycle. *Nature*, *419*(6903), 228–232. https://doi.org/10.1038/nature01092

Aryal, A., Shrestha, S., & Babel, M. S. (2019). Quantifying the sources of uncertainty in an ensemble of hydrological climate-impact projections. *Theoretical and Applied Climatology*, *135*(1–2), 193–209. https://doi.org/10.1007/s00704-017-2359-3

Berg, P., Moseley, C., & Haerter, J. O. (2013). Strong increase in convective precipitation in response to higher temperatures. *Nature Geoscience*, *6*(3), 181–185. https://doi.org/10.1038/ngeo1731

Bhatta, B., Shrestha, S., Shrestha, P. K., & Talchabhadel, R. (2019). Evaluation and application of a SWAT model to assess the climate change impact on the hydrology of the Himalayan River Basin. *Catena*, *181*. https://doi.org/10.1016/j.catena.2019.104082

Bhatta, B., Shrestha, S., Shrestha, P. K., & Talchabhadel, R. (2020). Modelling the impact of past and future climate scenarios on streamflow in a highly mountainous watershed: A case study in the West Seti River Basin, Nepal. *Science of The Total Environment*, *740*, 140156. https://doi.org/10.1016/j.scitotenv.2020.140156

Bohlinger, P., & Sorteberg, A. (2018). A comprehensive view on trends in extreme precipitation in Nepal and their spatial distribution. *International Journal of Climatology*, *38*(4), 1833–1845. https://doi.org/10.1002/joc.5299

Cook, B. I., Mankin, J. S., Marvel, K., Williams, A. P., & Smerdon, J. E. (2020). Twenty-first Century Drought Projections in the CMIP6 Forcing Scenarios. *Earth's Future*, *8*(6), e2019EF001461. https://doi.org/10.1029/2019EF001461

Dahal, V., Bhattarai, R., Shakya, N. M., Talchabhadel, R., & Dugar, S. (2015). Estimating the impact of climate change on streamflow in Bagmati Watershed, Nepal. *American Society of Agricultural and Biological Engineers Annual International Meeting 2015*, *6*.

Dhaubanjar, S., Prasad Pandey, V., & Bharati, L. (2020). Climate futures for Western Nepal based on regional climate models in the CORDEX‐SA. *International Journal of Climatology*, *40*(4), 2201–2225. https://doi.org/10.1002/joc.6327

Donat, M. G., Lowry, A. L., Alexander, L. V., O'Gorman, P. A., & Maher, N. (2016). More extreme precipitation in the world's dry and wet regions. *Nature Climate Change*, *6*(5), 508–513. https://doi.org/10.1038/nclimate2941

Dore, M. H. I. (2005). Climate change and changes in global precipitation patterns: What do we know? *Environment International*, *31*(8), 1167–1181. https://doi.org/10.1016/j.envint.2005.03.004

Eyring, V., Bony, S., Meehl, G. A., Senior, C. A., Stevens, B., Stouffer, R. J., & Taylor, K. E. (2016). Overview of the Coupled Model Intercomparison Project Phase 6 (CMIP6) experimental design and organization. *Geoscientific Model Development*, *9*(5), 1937–1958. https://doi.org/10.5194/gmd-9-1937-2016

Fischer, E. M., & Knutti, R. (2016). Observed heavy precipitation increase confirms theory and early models. *Nature Climate Change*, *6*(11), 986–991. https://doi.org/10.1038/nclimate3110

Groisman, P. Y., Karl, T. R., Easterling, D. R., Knight, R. W., Jamason, P. F., Hennessy, K. J., Suppiah, R., Page, C. M., Wibig, J., Fortuniak, K., Razuvaev, V. N., Douglas, A., Førland, E., & Zhai, P. M. (1999). Changes in the probability of heavy precipitation: Important indicators of climatic change. In *Climatic Change* (Vol. 42, Issue 1, pp. 243–283). https://doi.org/10.1023/A:1005432803188

Gusain, A., Ghosh, S., & Karmakar, S. (2020). Added value of CMIP6 over CMIP5 models in simulating Indian summer monsoon rainfall. *Atmospheric Research*, *232*, 104680. https://doi.org/10.1016/j.atmosres.2019.104680

Hulme, M., Osborn, T. J., & Johns, T. C. (1998). Precipitation sensitivity to global warming: Comparison of observations with HadCM2 simulations. *Geophysical Research Letters*, *25*, 3379. https://doi.org/10.1029/98GL02562

Kadel, I., Yamazaki, T., Iwasaki, T., & Abdillah, M. R. (2018). Projection of future monsoon precipitation over the central Himalayas by CMIP5 models under warming scenarios. *Climate Research*, *75*, 1–21.

Kaini, S., Nepal, S., Pradhananga, S., Gardner, T., & Sharma, A. K. (2020). Representative general circulation models selection and downscaling of climate data for the transboundary Koshi river basin in China and Nepal. *International Journal of Climatology*, *40*(9), 4131–4149. https://doi.org/10.1002/joc.6447

Kansakar, S. R., Hannah, D. M., Gerrard, J., & Rees, G. (2004). Spatial pattern in the precipitation regime of Nepal. *International Journal of Climatology*, *24*(13), 1645–1659. https://doi.org/10.1002/joc.1098

Karki, R., Talchabhadel, R., Aalto, J., & Baidya, S. K. (2016). New climatic classification of Nepal. *Theoretical and Applied Climatology*, *125*(3–4), 799–808. https://doi.org/10.1007/s00704-015-1549-0

Kawai, H., Yukimoto, S., Koshiro, T., Oshima, N., Tanaka, T., Yoshimura, H., & Nagasawa, R. (2019). Significant improvement of cloud representation in the global climate model MRI-ESM2. *Geoscientific Model Development*, *12*(7), 2875–2897. https://doi.org/10.5194/gmd-12-2875-2019

Kharin, V. V., Zwiers, F. W., Zhang, X., & Wehner, M. (2013). Changes in temperature and precipitation extremes in the CMIP5 ensemble. *Climatic Change*, *119*(2), 345–357. https://doi.org/10.1007/s10584-013-0705-8

Klein-Tank, A. M. G., Peterson, T. C., Quadir, D. A., Dorji, S., Zou, X., Tang, H., Santhosh, K., Joshi, U. R., Jaswal, A. K., Kolli, R. K., Sikder, A. B., Deshpande, N. R., Revadekar, J. V, Yeleuova, K., Vandasheva, S., Faleyeva, M., Gomboluudev, P., Budhathoki, K. P., Hussain, A., … Spektorman, T. (2006). Changes in daily temperature and precipitation extremes in central and south Asia. *Journal of Geophysical Research-Atmospheres*, *111*(D16), doi:10.1029/2005JD006316. https://doi.org/10.1029/2005jd006316

Mishra, V., Bhatia, U., & Tiwari, A. D. (2020). Bias-corrected climate projections for South Asia from Coupled Model Intercomparison Project-6. *Scientific Data*, *7*(1), 338. https://doi.org/10.1038/s41597-020-00681-1

Myhre, G., Alterskjær, K., Stjern, C. W., Hodnebrog, Ø., Marelle, L., Samset, B. H., Sillmann, J., Schaller, N., Fischer, E., Schulz, M., & Stohl, A. (2019). Frequency of extreme precipitation increases extensively with event rareness under global warming. *Scientific Reports*, *9*(1), 16063. https://doi.org/10.1038/s41598-019-52277-4

Pandey, V. P., Dhaubanjar, S., Bharati, L., & Thapa, B. R. (2019). Hydrological response of Chamelia watershed in Mahakali Basin to climate change. *Science of the Total Environment*, *650*, 365–383. https://doi.org/10.1016/j.scitotenv.2018.09.053

Pandey, V. P., Dhaubanjar, S., Bharati, L., & Thapa, B. R. (2020). Spatio-temporal distribution of water availability in Karnali-Mohana Basin, Western Nepal: Climate change impact assessment (Part-B). *Journal of Hydrology: Regional Studies*, *29*(December 2019), 100691. https://doi.org/10.1016/j.ejrh.2020.100691

Pincus, R., Batstone, C. P., Hofmann, R. J. P., Taylor, K. E., & Glecker, P. J. (2008). Evaluating the present-day simulation of clouds, precipitation, and radiation in climate models. *Journal of Geophysical Research*, *113*(D14), D14209. https://doi.org/10.1029/2007JD009334

Rajbhandari, R., Shrestha, A. B., Nepal, S., & Wahid, S. (2016). Projection of Future Climate over the Koshi River Basin Based on CMIP5 GCMs. *Atmospheric and Climate Sciences*, *06*(02), 190–204. https://doi.org/10.4236/acs.2016.62017

Schaller, N., Mahlstein, I., Cermak, J., & Knutti, R. (2011). Analyzing precipitation projections: A comparison of different approaches to climate model evaluation. *Journal of Geophysical Research*, *116*(D10), D10118. https://doi.org/10.1029/2010JD014963

Swart, N. C., Cole, J. N. S., Kharin, V. V., Lazare, M., Scinocca, J. F., Gillett, N. P., Anstey, J., Arora, V., Christian, J. R., Hanna, S., Jiao, Y., Lee, W. G., Majaess, F., Saenko, O. A., Seiler, C., Seinen, C., Shao, A., Sigmond, M., Solheim, L., … Winter, B. (2019). The Canadian Earth System Model version 5 (CanESM5.0.3). *Geoscientific Model Development*, *12*(11), 4823–4873. https://doi.org/10.5194/gmd-12-4823-2019

Talchabhadel, R., Aryal, A., Kawaike, K., Yamanoi, K., & Nakagawa, H. (2020). A comprehensive analysis of projected changes of extreme precipitation indices in West Rapti River basin, Nepal under changing climate. *International Journal of Climatology*, joc.6866. https://doi.org/10.1002/joc.6866

Talchabhadel, R., Karki, R., Thapa, B. R., Maharjan, M., & Parajuli, B. (2018). Spatio-temporal variability of extreme precipitation in Nepal. *International Journal of Climatology*, *38*(11), 4296–4313. https://doi.org/10.1002/joc.5669

Trenberth, K. E. (2011). Changes in precipitation with climate change. *Climate Research*, *47*(1), 123–138. https://doi.org/10.3354/cr00953

Trenberth, K. E., Dai, A., Rasmussen, R. M., & Parsons, D. B. (2003). The Changing Character of Precipitation. *Bulletin of the American Meteorological Society*, *84*(9), 1205–1218. https://doi.org/10.1175/BAMS-84-9-1205

Turner, A. G., & Annamalai, H. (2012). Climate change and the South Asian summer monsoon. *Nature Climate Change*, *2*(8), 587–595. https://doi.org/10.1038/nclimate1495

Vecchi, G. A., & Soden, B. J. (2007). Global Warming and the Weakening of the Tropical Circulation. *Journal of Climate*, *20*(17), 4316–4340. https://doi.org/10.1175/JCLI4258.1

Wentz, F. J., Ricciardulli, L., Hilburn, K., & Mears, C. (2007). How Much More Rain Will Global Warming Bring? *Science*, *317*(5835), 233–235. https://doi.org/10.1126/science.1140746

Wu, T., Lu, Y., Fang, Y., Xin, X., Li, L., Li, W., Jie, W., Zhang, J., Liu, Y., Zhang, L., Zhang, F., Zhang, Y., Wu, F., Li, J., Chu, M., Wang, Z., Shi, X., Liu, X., Wei, M., … Liu, X. (2019). The Beijing Climate Center Climate System Model (BCC-CSM): the main progress from CMIP5 to CMIP6. *Geoscientific Model Development*, *12*(4), 1573–1600. https://doi.org/10.5194/gmd-12-1573-2019

Yukimoto, S., Kawai, H., Koshiro, T., Oshima, N., Yoshida, K., Urakawa, S., Tsujino, H., DEUSHI, M., TANAKA, T., HOSAKA, M., YABU, S., YOSHIMURA, H., SHINDO, E., MIZUTA, R., OBATA, A., ADACHI, Y., & ISHII, M. (2019). The Meteorological Research Institute Earth System Model Version 2.0, MRI-ESM2.0: Description and Basic Evaluation of the Physical Component. *Journal of the Meteorological Society of Japan. Ser. II*, *97*(5), 931–965. https://doi.org/10.2151/jmsj.2019-051